Three Methods to Look at Walsh-type Diagrams Including Nuclear Repulsions*+

Yuuzi TAKAHATA† and Robert G. PARR

Department of Chemistry, The Johns Hopkins University, Baltimore, Maryland 21218, U.S.A.

(Received October 21, 1973)

Energy correlation diagrams for molecules of type AH_2 are examined by three different methods: (1) the quantum-mechanical virial theorem, (2) the method of median partition, (3) the integral Hellmann-Feynman theorem. Nuclear-nuclear repulsions are included. The formula for the first method takes the form $W=-\sum t_i$, where t_i is an orbital kinetic energy. The theory is applied to H_2O, CH_2, and BeH_2. Negative-kinetic-energies-*versus*-angle diagrams for these molecules are presented. The pattern of the diagrams is quite different from the usual Walsh diagram. With this resolution non-bonding electrons play a significant role in determining bond angles. In the second method the resolution of the total energy takes the form $W=\sum_i[e_i+V_n(i)]$, where e_i is a median electronic energy and $V_n(i)$ is a resolved nuclear repulsion energy calculated from an expression derived from ideas of population analysis. The energies-*versus*-angle diagram thus obtained for H_2O is similar to the one obtained by the first method. For the third method, the integral Hellmann-Feynman formula for the electronic energy change on bending is written in terms of corresponding orbital contributions, $\Delta E_l=\sum_i \Delta E_l(i)$, and nuclear-nuclear repulsion is added in a resolved form. For H_2O the ΔE_l resemble Walsh diagrams closely, both with and without the nuclear-nuclear repulsion increments. Wave functions used throughout are LCAO-SCF functions built from medium-size Gaussian basis sets.

Much effort has been dedicated to elucidate numerical rules governing molecular shapes, since Walsh first pointed out the existence of such rules for large number of simple polyatomic molecules.[1] There are two schools of thought in explaining the rules, valence bond theory and molecular orbital theory. It has been shown that the valence-shell electron pair repulsion theory (VSEPR) can explain Walsh's rules.[2] More recently it has been argued that closed shells on terminal atoms play an important role in the bending process, and a model has been given which predicts Walsh's magic numbers.[3,4] Connections between the model and the crystal field theory were noted.

Most quantum mechanical explanations of Walsh's rules have followed the lines laid by Mulliken[5] and Walsh.[1] Molecular orbital theory has been extensively applied giving "Walsh Diagrams."[6] United-atom approaches have also been applied producing Walsh-type diagrams.[7] It has remained a matter of argument, however, whether one should use the LCAO-MO-SCF orbital energies or some other one-electron MO energy quantities which genuinely add to give the total electronic energy in order to identify the Walsh ordinate.[8] There is another difficulty in the MO approach; Nuclear-nuclear repulsion has almost always been left out of consideration in calculating a Walsh diagram or at most added at the end.

In the present paper we explore the possibilities of obtaining method which enable one to partition the *total* molecular orbital energy of a molecule into one-electron energy quantities which are genuinely additive. Three schemes are employed for this purpose. They are the quantum-mechanical virial theorem, the method of median partition, and the integral Hellmann-Feynman theorem. The first method has already been applied by us to the H_2O molecule.[9] The energy correlation diagram obtained differed very much from the Walsh diagram. In Section II numerical results of further calculations on H_2O are presented, and the theorem is also applied to CH_2 and BeH_2. The second method follows closely the work of Coulson and Neilson[10] except that nuclear-nuclear repulsion energy is divided and included in the individual orbital components. The third method is of interest since it parallels the analysis of the same problem with the Hellmann-Feynman theorem, by Coulson and Deb.[8]

I. Wave Functions

Throughout this work we use single-determinantal linear combinations of Gaussian-type orbitals (LCGTO) SCF wave functions. A medium-size Gaussian basis set $(53/3)^{11a)}$ is employed for H_2O, while basis sets $(73/3)^{11b)}$ and $(53/3)^{11c)}$ are used for CH_2 and BeH_2 respectively. Gaussian exponents are tabulated in Table 1. LCGTO–SCF calculations are carried out at various bond angles and bond distances. The calculated equilibrium geometry H_2O has bond length 1.85 a.u. and bond angle of 112°, the corresponding experimental values being 1.8103 a.u. and 105°.

In the calculations reported in Section II below, the variation of bond distances with bond angle are considered, as described there. In the diagrams in Sections III and IV, on the other hand, the bond distances are held constant with change in bond angle.

II. Correlation Diagrams from the Quantum-mechanical Virial Theorem

It has already been pointed out that the polyatomic virial theorem in the form given by Nelander[12] gives theoretically rigorous correlation diagrams.[9] The central result of the Nelander theorem is that the relation $W=-T$ holds between the total energy W

* Aided by research grants to The Johns Hopkins University from the National Institutes of Health and the Pertroleum Research Fund of the American Chemical Socity.

+ Based on a thesis submitted by Yuuzi Takahata in partial fulfillment of the requirements for the degree of Doctor of Philosophy, The Johns Hopkins University, 1970.

† Present address: Department of Material Science, University of Electro-Communications, 1-5-1, Chofugaoka, Chofu-shi, Tokyo, Japan.

Table 1. Gaussian basis set for H_2O, CH_2, and BeH_2

Molecule	Center	Type	Exponents
	O	S	378.00
			74.5
			14.7
			2.89
			0.57
H_2O			
		P	9.38
			1.81
			0.35
	H	S	4.24
			0.658
			0.148
	C	S	994.9
			160.6
			39.91
			11.82
			3.698
			0.6026
			0.1817
CH_2			
		P	4.279
			0.8669
			0.2036
	H	S	6.4805
			0.9810
			0.2180
	Be	S	78.615
			15.524
			3.054
			0.600
			0.118
BeH_2		P	
			0.384
			0.074
	H	S	5.740
			0.775
			0.159

and the total kinetic energy T not only at the equilibrium geometry of a polyatomic molecule, but also for bond angles distorted from equilibrium, if the bond distances are optimum for each set of angles. Since kinetic energy is a one-electron quantity in the Hartree-Fock scheme, the total energy may be expressed as a sum of negative orbital kinetic energies:

$$W = \Sigma_i(-t_i). \quad (1)$$

This seems to be the only known theory which makes it possible to partition the total energy (including nuclear-nuclear repulsion) into genuinely additive one-electron componets. No nuclear-nuclear repulsion or electron-electron terms appear in the expression.

For approximate wave functions, the virial theorem as just stated does not hold unless the wave functions are scaled. The scaling procedure for polyatomic molecules may be patterned after Löwdin's treatment for diatomic molecules.[13]

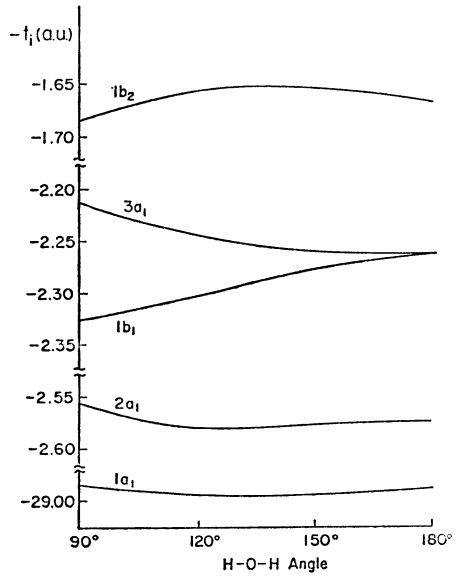

Fig. 1. Negative kinetic energies of the molecular orbitals of H_2O, as a function of H-O-H angle. See text.

In Table 2 are shown scaling factors (η), equilibrium bond lengths (R_e), kinetic (T), potential ($V=V_{ne}+V_{ee}$), nuclear repulsion (V_{nn}), and total (W) energies at various bond angles for H_2O. Note that the total energies are indeed equal to negative kinetic energies. The kinetic energies partitioned into one-electron components are listed in Table 3. These are plotted in Fig. 1 as a function of HOH angle.[9]

Figure 1 differs from a conventional Walsh diagram in two respects; (1) The order of the top three orbitals: $(1b_2)>(3a_1)>(1b_1)$, *versus* $(1b_1)>(3a_1)>(1b_2)$ in the conventional Walsh diagram, (2) The trends in changes of orbital energies differ. The $3a_1$ orbital energy component, for example, decreases with increasing apex angle in our diagram, whereas it increases in Walsh's.[1] The $1b_1$ orbital energy increases in Fig. 1, it remains constant in the Walsh diagram; *etc.*

We may note that the kinetic-energy-*versus*-angle diagram in Fig. 1 appears almost identical qualitatively with that of Coulson and Neilson,[10] who obtained their diagram by an entirely different method; see Section III below.

Earlier we argued,[9] by considering the diagram corresponding to Fig. 1 which is obtained by a certain unitary transformation of the orbitals, that lone-pair kinetic energies dominate the determination of geometry. The previously given evidence was basis-set dependent, but the conclusion may survive with accurate molecular orbitals if one makes an appropriate definition of the localization process—we do not know.

We next consider the molecule CH_2, in its $^1A_1$ state. This species has six valence electrons, and according to the Walsh rules it should be bent. In Fig. 2 are plotted the negative kinetic energies of CH_2 as functions of the HCH angle. If the figure is compared with the corresponding diagram for H_2O, Fig. 1, it can be seen that the same order of orbital (negative) kinetic energies prevails: $1b_2>3a_1>2a_1>1a_1$. However,

TABLE 2. SCALED QUANTITIES FOR H_2O

Scaling factors η, equilibrium bond distances R_e, scaled electronic kinetic (T), potential (V) energies, nuclear repulsion energies V_{nn}, total energies W.

θ	η	R_e	T	$V=V_{ne}+V_{ee}$	V_{nn}	W
90°	1.0015	1.8651	75.5373	−151.0747	8.9577	−75.5373
105°	1.0016	1.8442	75.5508	−151.1016	9.0176	−75.5507
130°	1.0017	1.8189	75.5458	−151.0916	9.0840	−75.5458
150°	1.0018	1.8034	75.5301	−151.0603	9.1590	−75.5301
180°	1.0018	1.7811	75.5171	−151.0342	9.2639	−75.5171

TABLE 3. MOLECULAR ORBITAL KINETIC ENERGIES t_i FOR H_2O

θ	Orbital					Total
	$1a_1$	$2a_1$	$3a_1$	$1b_2$	$1b_1$	
90°	28.9852	2.5551	2.2146	1.6871	2.3267	75.5378
105°	28.9913	2.5709	2.2311	1.6661	2.3159	75.5506
130°	28.9949	2.5789	2.2510	1.6541	2.2942	75.5458
150°	28.9963	2.5765	2.2605	1.6551	2.2766	75.5302
180°	28.9893	2.5731	2.2632	1.6697	2.2632	75.5170

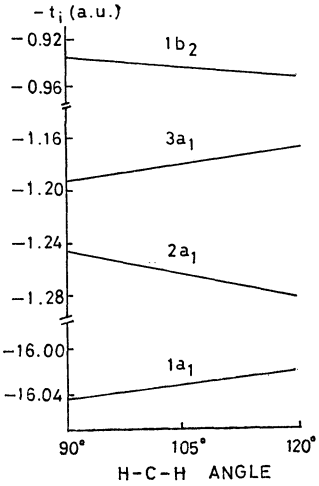

Fig. 2. Negative kinetic energies of the molecular orbitals of CH_2.

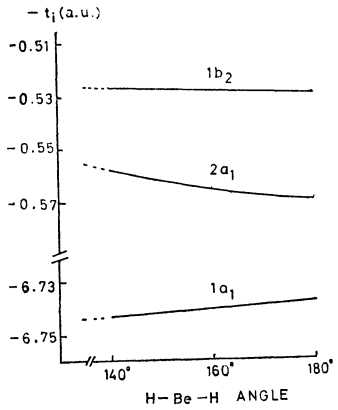

Fig. 3. Negative kinetic energies of the molecular orbitals of BeH_2.

energy changes with angle of individual orbitals are not the same in the two cases.

In Fig. 3 are plotted the corresponding orbital kinetic energies for BeH_2. The two top curves show minima at 180°, which may be regarded as showing how the four valence electrons drive the molecule linear.. This could be considered to be an explanation of one of the Walsh rules, which states that AH_2 molecules containing four valence electrons are linear. In the Figure it is seen that, indeed, the two bonding orbitals, $1b_2$ and $2a_1$, favor a linear conformation. This kinetic energy correlation diagram accounts for the shape of BeH_2. The orbital which contributes most in determining the molecular shape is $2a_1$.

Comparisons among the kinetic energy diagrams of H_2O, CH_2, and BeH_2 reveal that the kinetic diagram varies from one molecule to another—there seems to be no universal kinetic energy diagram. However, the kinetic diagrams do contain information about the roles played by the various orbitals, and they certainly do correspond to a rigorous resolution of the energy into components.

III. Correlation Diagrams from the Method of Median Partition

A true energy-angle correlation diagram must take into account all effects which occur on changing bond-angles, including nuclear-nuclear repulsion changes. The application of the virial theorem is an *indirect* method to include the nuclear repulsion energy; in this section we search for a possibility of including nuclear-nuclear repulsion directly. The question is how the total energy W can be resolved into additive parts $w(i)$ such that $W=\sum_i w(i)$. With $W=E+V_{nn}$, the problem is to find methods which partition both E and V_{nn} into additive parts.

First we consider the partition of the electronic energy E. In the Hartree-Fock approximation the additive resolution of E was discussed as early as 1951 in connection with semi-empirical calculations with the LACO-MO method; namely,

$$E = \sum_{\text{occupied MO's}}(\varepsilon_i + I_i) = 2\sum_i m_i \tag{2}$$

where I_i is the core integral $\int \phi_i^* H_{\text{core}} \phi_i d\tau'$ of the molecular orbital ϕ_i, and

$$m_i = 1/2(\varepsilon_i + I_i) = 1/2e_i. \tag{3}$$

The quantity m_i has been called the *median one-electron energy* or simply median energy.[14]

In 1963 Coulson and Neilson suggested the use of the median energies m_i in obtaining Walsh diagrams.[10] They rejected the use of the Hartree-Fock orbital energies ε_i for that purpose on the basis that ε_i are not truly additive. The Walsh diagram of median energies for the water molecule H_2O reported by Coulson and Neilson differs significantly from the diagram of orbital energies. Since then the use of the median energies m_i for a Walsh diagram has been a matter of controversy. Yet Eq. (2) is a resolution, which is truly additive of the total electronic energy, and we will use this in this section.

The task left is how to partition V_{nn} into additive parts. Coulson and Neilson did not address this problem.

Consider a diatomic molecule AB with nuclear charges Z_A and Z_B. Let N_A and N_B be gross atomic populations according to Mulliken's definition,[15] on atoms A and B, respectively. $N(i, A)$ and $N(i, B)$ are subtotal populations in molecular orbital ϕ_i on A and B, and related to N_A and N_B by $N_A = \sum_i N(i,A)$, and $N_B = \sum_i N(i, B)$. The nuclear-nuclear repulsion energy V_{nn} of AB is exactly $V_{nn} = Z_A Z_B / R$, where R is the bond length of the molecule. V_{nn} is related to N_A and N_B by the formula

$$\begin{aligned} V_{nn} &= \frac{1}{R}[(Z_A - N_A)(Z_B - N_B) + (Z_A N_B + Z_B N_A) - N_A N_B] \\ &= \frac{1}{R}[(Z_B - 1/2N_B)N_A + (Z_A - 1/2N_A)N_B] \\ &\quad + \frac{1}{R}(Z_A - N_A)(Z_B - N_B). \end{aligned} \tag{4}$$

Let us assume that the second term of Eq. (4) is much smaller than the first term, call it Δ. Then V_{nn} is given by,

$$\begin{aligned} V_{nn} &= \frac{1}{R}[(Z_B - 1/2N_B)N_A + (Z_A - 1/2N_A)N_B] + \Delta \\ &= \sum_i \frac{1}{R}[(Z_B - 1/2N_B)N(i,A) + (Z_A - 1/2N_A)N(i,B)] + \Delta \\ &= \sum_i \left[V_n'(i) + \frac{V_n'(i)}{\sum_i V_n'(i)} \Delta \right] = \sum_i V_n(i) \end{aligned} \tag{5}$$

where

$$V_n'(i) = \frac{1}{R}[(Z_B - 1/2N_B)N(i,A) + (Z_A - 1/2N_A)N(i,B)]. \tag{6}$$

The quantity Δ vanishes when $Z_A = N_A$ or $Z_B = N_B$. This happens whenever $Z_A = Z_B$. The quantity in the bracket of Eq. (5),

$$V_n(i) = V_n'(i) + \frac{V_n'(i)}{\sum_i V_n'(i)} \Delta, \tag{7}$$

defines the i-th component of the partitioned V_{nn}.

For polyatomic molecules, the foregoing partitioning method may be applied to each contribution to the nuclear repulsion energy. For instance the nuclear repulsion energy of a molecule AH_2 is the sum of two terms as follows,

$$\begin{aligned} V_{nn} &= 2\frac{Z_A Z_H}{R_{AH}} + \frac{Z_H^2}{R_H} \\ &= 2\sum_i \frac{1}{R_{AH}}[(Z_H - 1/2N_H)N(i,A) + (Z_A - 1/2N_A)N(i,H)] \\ &\quad + \sum_i \frac{1}{R_H}[(Z_H - 1/2N_H)N(i,H) \\ &\quad + (Z_H - 1/2N_H)N(i,H)] + \Delta \\ &= \sum_i [2V_{AH}'(i) + V_{HH}'(i)] + \Delta \\ &= \sum_i \left[V_n'(i) + \frac{V_n'(i)}{\sum V_n'(i)} \Delta \right] = \sum_i V_n(i), \end{aligned} \tag{8}$$

where

$$V_{AH}'(i) = \frac{1}{R_{AH}}[(Z_H - 1/2N_H)N(i,A) + (Z_A - 1/2N_A)N(i,H)], \tag{9}$$

$$V_{HH}'(i) = \frac{2}{R_H}(Z_H - 1/2N_H)N(i,H), \tag{10}$$

and

$$V_n(i) = 2V_{AH}'(i) + V_{HH}'(i) + \frac{V_n'(i)}{\sum V_n'(i)} \Delta. \tag{11}$$

For the total energy, from Eq. (2) and Eq. (8) we have a rigorous partitioning,

$$W = E + V_{nn} = \sum_{\text{occupied MO's}} [\varepsilon_i + I_i + V_n(i)] = \sum_i w(i) \tag{12}$$

where

$$w(i) = \varepsilon_i + I_i + V_n(i). \tag{13}$$

The partitioned nuclear energies in H_2O are tabulated in Table 4. In Table 5 are presented the quantities $w(i)$. The sum $\sum w(i)$ in Table 5 does not necessarily agree with W in Table 3, since the bond distances are fixed to 1.8103 in Table 5 whereas in Table 2 they are varied to satisfy Eq. (1).

In Fig. 4 is given the correlation diagram obtained

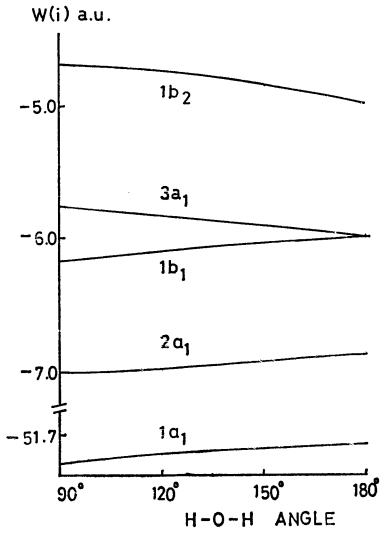

Fig. 4. Energy components for the different molecular orbitals in H_2O — Eqs. (12) and (13) of text.

Table 4. Partitioned nuclear repulsion energies $V_n(i)$ for H_2O

θ	$V_n(i)$					$\sum V_n(i)$
	$1a_1$	$2a_1$	$3a_1$	$1b_2$	$1b_1$	
90°	1.43267	2.10801	1.74001	2.51846	1.42977	9.22892
105°	1.44428	2.08528	1.67666	2.53868	1.44155	9.18645
110°	1.44890	2.08218	1.65972	2.53847	1.44623	9.17549
130°	1.47407	2.08421	1.60254	2.51059	1.47164	9.14306
150°	1.50721	2.09869	1.55957	2.45382	1.50496	9.12424
180°	1.53645	2.11302	1.53434	2.39635	1.53434	9.11450

Table 5. Partitioned total energy components $w(i)$ for H_2O

θ	$w(i)$					$\sum w(i)$
	$1a_1$	$2a_1$	$3a_1$	$1b_2$	$1b_1$	
90°	−51.9021	−7.03109	−5.75927	−4.67812	−6.16456	−75.5351
105°	−51.8810	−7.02489	−5.80927	−4.69610	−6.13834	−75.5496
110°	−51.8727	−7.01751	−5.82285	−4.71020	−6.12806	−75.5513
130°	−51.8303	−6.97196	−5.87446	−4.79132	−6.0773	−75.5453
150°	−51.7791	−6.91668	−5.9264	−4.89046	−6.01703	−75.5297
180°	−51.7356	−6.87195	−5.96618	−4.97592	−5.96618	−75.5159

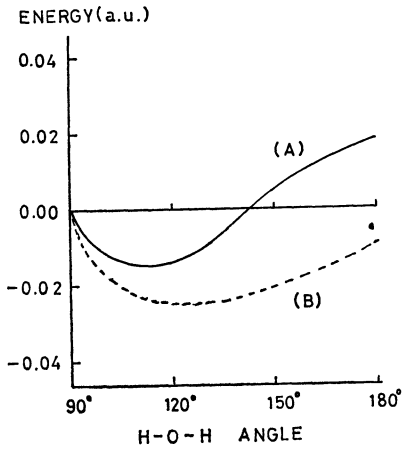

Fig. 5. (A) Total relative energy of H_2O. (B) Lone pair relative energies in H_2O. See text.

by plotting $w(i)$ *versus* bond angle. If Fig. 4 is compared with Fig. 1, it is noticed that the order and the patterns of the curves are similar in the two figures. The coincidences prevailing among the figures are remarkable because they are obtained by entirely different methods of partition.

It is interesting to see how the "lone pair" energies $[w(3a_1)+w(1b_1)]$ change with θ. In Fig. 5 are plotted the relative lone pair energies and the total energy with the reference angle $\theta=90°$. The "lone pair" energies are seen to monitor the total energy W. We previously found a similar result when the quantum-mechanical virial theorem was applied for partitioning W.[9] The implication again is that lone pair electrons may control the equilibrium bond angle in H_2O. Further investigation along this line is required.

The partitioned nuclear-nuclear repulsion components are relatively small in comparison with the electronic energy components, as seen in Tables 4 and 5. This implies that inclusion of the partitioned nuclear repulsion energies does not alter general appearance of correlation diagrams obtained without including nuclear repulsion.

It would be interesting to extend the present method of partitioning W to various diatomic molecules as well as to other polyatomic molecules, and to compare the correlation energy diagrams so obtained—energy-*versus*-bond length for diatomic molecules, energy-*versus*-bond angle for polyatomic molecules—with the traditional ones.

IV. Correlation Diagrams from Integral Hellmann-Feynman Theorem

An energy difference ΔW_l between two isoelectronic states X and Y may be obtained from the integral Helmann-Feynman Theorem (IHF):[16]

$$\Delta W_l = \int \Psi_X H' \Psi_Y d\tau \Big/ \int \Psi_X \Psi_Y d\tau \qquad (14)$$

where H' is the difference of the two Hamiltonian operators of states X and Y. If one defines the transition density between the two states X and Y by

$$\rho_{XY}(1) = \frac{N}{S}\int \Psi_X(12\cdots N)\ \Psi_Y(12\cdots N)\ d\tau(23\cdots N) \qquad (15)$$

then Eq. (14) becomes

$$\Delta W_l = \int \rho_{xy}(1) h(1) d\tau(1) + \Delta V_{nn}, \qquad (16)$$

where $h(1)$ is the change in the nuclear-electron attraction operator. This equation shows that the electronic energy difference is directly related to the transition density. Hence the IHF theorem admits a classical interpretation of an energy change.

If approximate wavefunctions Ψ_X and $\tilde{\Psi}_Y$ for states X and Y are specified as single Slater determinants built from one-electron orbitals ϕ_X and ϕ_Y, it is always

Table 6. Orbital contributions to the changes of total electronic energies of H_2O

θ	$[1a_1]$	$[2a_1]$	$[3a_1]$	$[1b_2]$	ΔE_t
105°	−0.00003	−0.02185	0.05925	−0.02704	0.020667
110°	−0.00004	−0.03025	0.07948	−0.03547	0.027443
130°	−0.00010	−0.06959	0.16357	−0.06652	0.054727
150°	−0.00013	−0.11969	0.25221	−0.08998	0.084818
180°	−0.00014	−0.08844	0.25470	−0.10122	0.129805

a) Energies relative to 90° bond angle. Bond distance 1.8103 Å.

Table 7. Resolved nuclear repulsion energy changes for H_2O[a)]

θ	$-\Delta V(1a_1)$	$-\Delta V(2a_1)$	$-\Delta V(3a_1)$	$-\Delta V(1b_2)$	$-\Delta V_{total}$
105°	0.00002	0.00143	0.01876	0.02219	0.04246
110°	0.00002	0.00166	0.02378	0.02787	0.05343
130°	0.00005	0.00192	0.0393	0.04426	0.08585
150°	0.00059	0.00215	0.0486	0.05308	0.10466
180°	0.00060	0.02000	0.03608	0.0567	0.11440

a) Relative to the 90° configuration.

Table 8. Resolved total energy changes for H_2O[a)]

θ	$\Delta W(1a_1)$	$\Delta W(2a_1)$	$\Delta W(3a_1)$	$\Delta W(1b_2)$	$\Delta W(1b_1)$	ΔW_i^{total}
105°	−0.00005	−0.02328	0.04049	−0.04923	0	−0.02179
110°	−0.00006	−0.03191	0.05570	−0.06334	0	−0.02599
130°	−0.00015	−0.07151	0.12427	−0.11078	0	−0.03112
150°	−0.00072	−0.12184	0.20361	−0.14306	0	−0.01984
180°	−0.00074	−0.10844	0.2187	−0.15792	0	0.01541

a) Relative to the 90° configuration.

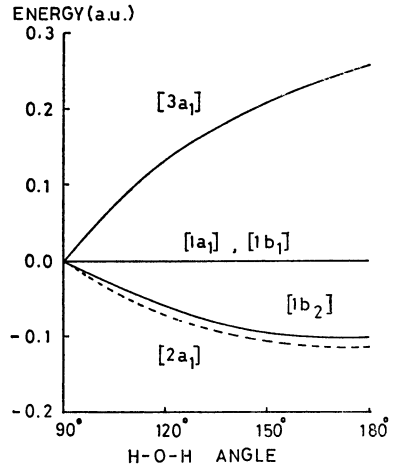

Fig. 6. Correlation diagram for H_2O obtained by the IHF theorem. Nuclear-nuclear repulsion is not included.

possible to find $\tilde{\Psi}'_X$ and $\tilde{\Psi}'_Y$ which diagonalize the transition density matrix by unitary transformations of $\tilde{\Psi}_X$ and $\tilde{\Psi}_Y$. It can be shown that Eq. (16) may be written[17)]

$$\Delta W_l = 2\sum_k^{N/2} \frac{\langle \hat{\phi}_k^X | h(1) | \hat{\phi}_k^Y \rangle}{\langle \hat{\phi}_k^X | \hat{\phi}_k^Y \rangle} + \Delta V_{nn} \qquad (17)$$

where $\hat{\phi}_k$'s are molecular orbitals from which Ψ''s are built. They are called corresponding orbitals. Equation (17) shows that the change of the total electronic energy ΔE_l can be expressed as a sum of the partitioned quantities $\Delta E(i) \equiv 2\langle \hat{\phi}_i^X | h(1) | \hat{\phi}_i^Y \rangle / \langle \hat{\phi}_i^X | \hat{\phi}_i^Y \rangle$. This is an equation which we may make use of to obtain energy-angle correlation diagrams for polyatomic molecules by plotting $\Delta E(i)$ as a function of bond angle.

Integral Hellmann-Ferynman calculations were carried out for the molecule H_2O to compute energy changes with changes of bond angles. In Table 6 are presented the results, for the symmetric bent in which two hydrogen atoms are moved symmetrically. They are plotted in Fig. 6 as functions of HOH angles. This is a *relative correlation* diagram because only relative electronic energies to that of HOH angle 90° are plotted.

From Fig. 6 we can see which orbital components favor linear conformations and which favor bent conformations, and so on. For instance $[3a_1]$ strongly favors the bent conformation for H_2O, whereas both $[1b_2]$ and $[2a_1]$ favor the linear conformation. The rest, $[1a_1]$ and $[1b_1]$, have little effect in determining the shape of the molecule. Thus the bent shape of H_2O may be attributed to the specific character of $[3a_1]$. This is in accord with Walsh's statement of the role played by the $3a_1$ orbital from the point of view of binding energy.[1)] If Fig. 6 is compared with the energy diagram of Walsh, an interesting feature is noticed: The *trends* of energy changes of individual orbital components coincide completely. In both diagrams $1a_1$ and $1b_1$ remain constant, $3a_1$ increases, $2a_1$

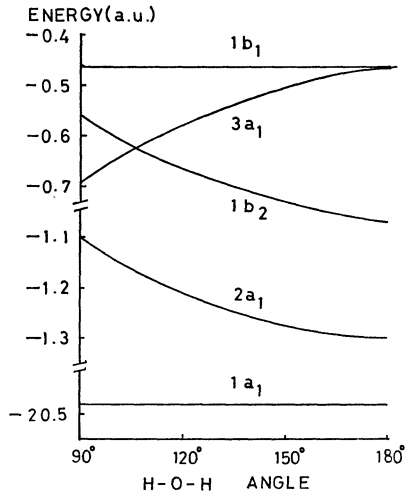

Fig. 7. Energy correlation diagram for H_2O including nuclear repulsion energies.

and $1b_2$ decrease as the bond angle increases from 90° to 180°.

Instead of using the IHF theorem, Coulson and Deb used the ordinary Hellmann-Feynman theorem, giving a new interpretation of the ordinate in the Walsh diagram.[8] Their force diagram looks similar to our IHF diagram except that $2a_1$ contribution rises in force diagram while it goes down in our diagram, as the bond angle increases.

So far the nuclear repulsion energies ΔV_{nn} have been left out, although clearly they should be taken into account in dealing with the problem of total energy change with conformational change. Resolution of ΔV_{nn} may be achieved in an analogous manner to the way V_{nn} was resolved in orbital components in Section III using corresponding orbitals and the method of population analysis of Mulliken with modifications. Because of close analogy between the two, detailed descriptions will not be given here. The resolved nuclear repulsion energies $\Delta V(i)$ are presented in Table 7.

The $\Delta V(i)$ may be divided into two classes: One is $\{[1a_1], [2a_1]$, and $[1b_1]\}$, the other is $\{[3a_1]$ and $[1b_2]\}$. The first class remains nearly constant with variations of bond angles, whereas the second changes very much more. The resolved nuclear energies $\Delta V(i)$ were added to the corresponding part of the electronic energies ΔE (i) to give total energy changes; these are listed in Table 8.

A *relative* correlation diagram such as Fig. 6 is useful when relative energy changes are concerned. However, it is desirable to have absolute correlation diagrams that show which orbital is higher in energy, and one comes next, and so on in treating Walsh's rules. If we assume a one to one correspondence between a Hartree-Fock molecular orbital and a corresponding orbital CMO in the IHF theory, $(1a_1)_{MO}$ *vs.* $[1a_1]_{CMO}$, $(2a_1)_{MO}$ *vs.* $[2a_1]_{CMO}$, $(3a_1)_{MO}$ *vs.* $[3a_1]_{CMO}$ *etc.*, and, assume that they have the same orbital energies at H–O–H angle 180°, an aboslute correlation diagram may be obtained, as in Fig. 7. If the correlation diagram in Fig. 7 is compared with the Walsh original diagram, a parallelism between the two figures is seen. Walsh's rules can be explained exactly as by Walsh if Fig. 7 is used.

The general trends of changes of one electron component stay more or less the same before and after inclusions of ΔV_{nn} terms, as seen in Figs. 6 and 7. This is another implication that *qualitative* Walsh-diagram may be obtained without taking ΔV_{nn} into consideration.

References

1) A. D. Walsh, *J. Chem. Soc.*, **1953**, 2260, 2266, 2288, 2296, 2301.
2) H. F. Thompson, *J. Amer. Chem. Soc.*, **93**, 4609 (1971).
3) Y. Takahata, G. Schnuelle, and R. G. Parr, *ibid.*, **93**, 784 (1971).
4) G. W. Schnuelle and R. G. Parr, *ibid.*, **94**, 8974 (1972).
5) R. S. Mulliken, *Rev. Mod. Phys.*, **14**, 204 (1942).
6) For example, S. D. Peyerimhoff, R. J. Buenker, and L. C. Allen, *J. Chem. Phys.*, **45**, 734 (1966).
7) C. E. Wulfman, *ibid.*, **31**, 381 (1959).
8) C. A. Coulson and B. M. Deb, *Int. J. Quant. Chem.*, **V**, 411 (1971).
9) Y. Takahata and R. G. Parr, *Chem. Phys. Lett.*, **4**, 109 (1969).
10) C. A. Coulson and A. H. Neilson, *Discuss. Faraday Soc.*, **35**, 71 (1963).
11) (a) J. W. Moscowitz and M. C. Harrison, *J. Chem. Phys.*, **43**, 3550 (1965); (b) D. R. Whitman, and C. J. Hornback, *ibid.*, **51**, 398 (1969); (c) M. C. Harrison and I. G. Csizmadia, MIT SSMTG, QPR, July 15, 1963.
12) B. Nelander, *J. Chem. Phys.*, **51**, 469 (1969).
13) P. O. Löwdin, *J. Mol. Spectrosc.*, **3**, 46 (1959).
14) R. G. Parr, *J. Chem. Phys.*, **19**, 799 (1951).
15) R. S. Mulliken, *ibid.*, **23**, 1833 (1955).
16) R. G. Parr, *ibid.*, **40**, 3726 (1964).
17) H. F. King, R. E. Stanton, H. Kim, R. F. Wyatt, and R. G. Parr, *ibid.*, **47**, 1936 (1967).